ELSEVIER

Computational Materials Science 29 (2004) 138–144

COMPUTATIONAL MATERIALS SCIENCE

www.elsevier.com/locate/commatsci

First-principles study of structural, dynamical, and dielectric properties of κ-Al_2O_3

R. Vali [a,b,*], S.M. Hosseini [a]

[a] *Department of Physics, Faculty of Sciences, Ferdowsi University of Mashhad, Iran*
[b] *School of Physics, Damghan University of Basic Sciences, P.O. Box 36715/364, Damghan, Iran*

Received 21 January 2003; received in revised form 30 April 2003; accepted 2 June 2003

Abstract

We have performed a first-principles study of the structural, dynamical, and dielectric properties of κ-Al_2O_3. The relaxed structural parameters are found to be in excellent agreement with experimental data. Using density-functional perturbation theory, we obtain the Born effective charge tensors, the phonon frequencies at the center of the Brillouin zone, and the electronic and static dielectric permittivity tensors of κ-Al_2O_3. Using our calculated results of κ-Al_2O_3, together with the previous theoretical results of α-Al_2O_3 and available experimental data of amorphous Al_2O_3, we demonstrate the coordination dependence of ionic contribution to static dielectric constant of Al_2O_3.

PACS: 77.22.−d; 63.20.−e; 61.66.−f
Keywords: κ-Al_2O_3; Density-functional theory; Dielectric permittivity tensors; Gate-dielectric

1. Introduction

Alumina, due to its hardness, abrasion resistance, corrosion resistance, mechanical strength, and good electrical insulation, is a material of high technological significance. A prospective application of particular current interest is its possible use to replace SiO_2 as the gate-dielectric material in metal-oxide–semiconductor (MOS) devices. As predicted by International Technology Roadmap for Semiconductor (ITRS), the scaling of complimentary MOS (CMOS) devices will come to an abrupt end around the year 2012 [1]. This will happen due to a high level of direct tunneling current, through the SiO_2 gate with a thickness below 20 Å, which would require a level of power dissipation that would be intolerable for most digital device application [2]. This problem is largely attributable to the low dielectric constant of SiO_2 ($\varepsilon \approx 3.9$). To overcome this problem, a high-k material is needed to replace SiO_2 gate-dielectric. Higher value of k allows the use of physically thicker films to obtain the same effective capacitance as in SiO_2 devices, and thus provides potential for significantly reduced direct tunneling. Any alternative gate-dielectric must satisfy several additional conditions, such as: thermal stability on Si surface, large band gap, and low degree of

* Corresponding author. Address: School of Physics, Damghan University of Basic Sciences, P.O. Box 36715/364, Damghan, Iran.
E-mail address: vali@dubs.ac.ir (R. Vali).

0927-0256/$ - see front matter © 2003 Published by Elsevier B.V.
doi:10.1016/j.commatsci.2003.06.009

dopant diffusion in the gate oxide. Some of the proposed candidates include ZrO_2 [3,4], HfO_2 [4], Al_2O_3 [4–7], La_2O_3 [8], Y_2O_3 [4,9], Gd_2O_3 [9], aluminates and silicates [10]. Although among these materials Al_2O_3 has relatively low gains in the dielectric constant relative to SiO_2, it has reasonably high band gap and can be deposited directly on Si without an interlayer, and has a very good thermal robustness [4]. Also, due to the existence of a knowledge base of this material in CVD processing in the history of semiconductor industry, it can be considered as a near-term material. In addition, since by using Al_2O_3 as the starting material, aluminates can be studied as alternative gate-dielectric, the study of this material is desirable. As far as we know, a first-principles study on dielectric properties of κ-Al_2O_3 has not yet been done. Of course, the research community is exploring amorphous alumina as a replacement high-k gate-dielectric material. However, density-functional theory calculation primarily uses periodic systems. Hence, we use kappa phase of alumina that has metal bonding and coordination similar to amorphous phase of alumina. Both phases contain Al atoms in both tetrahedral and octahedral coordination to O atoms [11,12]. Using density-functional theory, first we study the atomic structure of κ-Al_2O_3. The relaxed atomic structure is found in excellent agreement with the experimental one [11]. We use density-functional perturbation theory to compute the linear response functions such as: the Born effective charge tensors, zone center phonon frequencies, and the electronic and static dielectric permittivity tensors of κ-Al_2O_3. The paper is organized as follows. Section 2 describes the technical aspects of our first-principles calculations. Section 3 presents the results, including the structural parameters and linear response functions such as: the Born effective charge tensors, the zone center phonon frequencies, and the electronic and static dielectric permittivity tensors. Section 4 concludes the paper.

2. Details of first-principles calculations

The present calculations are performed with use of the ABINIT code [13], which is based on first-principles pseudopotentials and plane waves in the framework of the density-functional theory [14]. It relies on an efficient fast Fourier transform algorithm [15] for the conversion of wave functions between real and reciprocal spaces, on an adaptation to a fixed potential of the band-by-band conjugate-gradient method [16], and on a potential based conjugate-gradient algorithm [17] for the determination of the self-consistent potential. The exchange-correlation energy is evaluated within the local-density approximation [18] by using Ceperley–Alder homogeneous electron gas data [19]. The all electron potentials are replaced by norm conserving pseudopotentials [20,21] with Al(3s,3p), O(2s,2p) levels treated as valence states. The wavefunctions are expanded in plane wave up to a kinetic energy cutoff of 36 Ha. The Brillouin zone is sampled by a $4\times2\times2$ Monkhorst–Pack [22] mesh of k points. Both kinetic energy cutoff and k-point sampling are found to provide sufficient precision in present calculations. A unit cell containing 40 atoms (16 Al and 24 O atoms) is used in our calculations. The linear response functions such as the Born effective charge tensors, the zone center phonon frequencies, and the electronic and static dielectric permittivity tensors have been computed within a variational formulation of the density-functional perturbation theory [23–26]. In response function calculation we used the same parameters as for the calculation of the ground state properties.

3. Results

3.1. Atomic structure

The crystal structure of κ-Al_2O_3 is orthorhombic of point group $pna2_1$ with 8 formula units per primitive unit cell. In terms of coordination polyhedral it can be described as an ABAC closed-packed stacking of O atoms, with Al atoms occupying octahedral and tetrahedral sites. The number of octahedral and tetrahedral Al atoms in a unit cell is 12 and 4, respectively. The crystal fourfold symmetry (mm2) results in 10 independent atoms positions: 6O, 3 octahedral Al and 1 tetrahedral Al. These 10 independent sites are

replicated with the Wyckoff positions of A (x, y, z), B $(-x, -y, z + 1/2)$, C $(x + 1/2, -y + 1/2, z)$ and D $(-x + 1/2, y + 1/2, z + 1/2)$ to yield the 40 atom positions in the unit cell. Table 1 summarizes the results obtained after structural relaxation as well as results of experimental work [11] for comparison. We use the experimental parameters given in Table 1 as the starting point for structural relaxation, and we also checked that the residual forces on each atom after relaxation to be less than 10^{-2} eV/Å. The calculated lattice constants a, b, and c as well as internal parameters are found to be in excellent agreement with their corresponding experimental values [11]. The very close (usually <1%) agreement with the experimental values provides a good confirmation of the reliability of our calculations and this is sufficient to allow further study of the linear response properties.

3.2. Linear response functions

The static dielectric permittivity tensor (ε_0) can be separated into electronic and ionic contributions. The electronic contribution (ε_∞) arises from purely electronic screening and can be obtained as second derivative of the energy of the electronic system with respect to electric field. We find

$$\begin{pmatrix} 3.185 & 0 & 0 \\ 0 & 3.167 & 0 \\ 0 & 0 & 3.150 \end{pmatrix} \quad (1)$$

This tensor is diagonal and has the correct form expected from the crystal point group.

The calculation of the lattice contribution to the static dielectric permittivity tensor entails the computation of the Born effective charge tensors $Z^*_{\kappa,\alpha\beta}$ are defined as the force in the direction α on the atom κ due to an homogeneous unitary electric field along the direction β, or equivalently, as the induced polarization of the solid along the direction α by a unit displacement in the direction β of the atomic sublattice. Within variational formulation of density-functional perturbation theory they can be obtained as second derivative of total energy with respect to atomic displacement or to an external electric field. Our results for the Born effective charge tensors of the 10 independent atoms are presented in Table 2. The effective charge tensors for every other atom can be obtained using the symmetry operation of the crystal system. The presence of six non-equivalent oxygen atoms is reflected in the differences between their Born effective charge tensors. Also the Born effective charge tensors of the four Al atoms are different and this is a reflection of their non-

Table 1
Calculated structural parameters of κ-Al_2O_3 compared to experimental values (Ref. [11])

	This work			Experiment		
Lattice constants						
a	4.8042			4.8437		
b	8.2620			8.3300		
c	8.8816			8.9547		
Internal parameters						
	x	y	z	x	y	z
Al(1)	0.6839	0.8400	0.0043	0.6787	0.8416	0
Al(2)	0.1868	0.3462	0.7827	0.1846	0.3432	0.7868
Al(3)	0.8222	0.6520	0.6956	0.8115	0.6489	0.6972
Al(4)	0.6734	0.4687	0.9947	0.6677	0.4696	0.9993
O(1)	0.3434	0.8390	0.8944	0.3290	0.8313	0.8927
O(2)	0.0215	0.4881	0.6301	0.0248	0.4908	0.6292
O(3)	0.4806	0.6687	0.6361	0.4717	0.6647	0.6381
O(4)	0.5202	0.6757	0.1238	0.5145	0.6728	0.1212
O(5)	0.8439	0.3313	0.8688	0.8608	0.3301	0.8662
O(6)	0.3435	0.4992	0.9000	0.3360	0.4992	0.9000

Lattice constants a, b, c are in Å and internal coordinates x, y, and z are dimensionless.

Table 2
Calculated Born effective charge tensors for 10 independent atoms in κ-Al_2O_3

	Al(1)	Al(2)	Al(3)	Al(4)	O(1)	O(2)	O(3)	O(4)	O(5)	O(6)
xx	3.05	3.00	2.73	2.98	−1.86	−1.90	−1.93	−2.17	−1.94	−1.95
xy	−0.07	−0.06	−0.02	0.06	−0.01	0.09	0.07	0.09	−0.03	0.00
xz	0.00	0.06	−0.01	−0.07	−0.02	0.00	−0.14	−0.12	0.20	−0.18
yx	−0.07	0.00	0.01	0.08	0.02	0.05	0.08	0.10	−0.06	0.02
yy	2.86	2.89	2.82	3.09	−1.89	−2.00	−1.93	−1.93	−1.95	−1.95
yz	0.00	0.14	0.00	0.09	0.05	−0.06	−0.28	−0.18	−0.33	−0.34
zx	0.03	0.03	0.00	−0.03	−0.01	0.05	−0.14	−0.14	0.15	−0.16
zy	−0.06	0.09	0.01	0.06	0.07	−0.06	−0.32	−0.16	−0.29	−0.34
zz	2.67	3.06	2.89	2.86	−2.11	−1.93	−1.72	−2.03	−1.86	−1.83

equivalency. However from Table 2 it is obvious that the diagonal elements of the Born effective charge tensors obtained for all atoms are nearly close to their nominal ionic valence and the amplitude of the off-diagonal elements are small. This is in agreement with the nearly ionic picture of this system.

The squares of phonon frequencies at zone center are obtained as eigenvalues of the dynamical matrix

$$\widetilde{D}_{\kappa\alpha,\kappa'\beta} = \widetilde{C}_{\kappa\alpha,\kappa'\beta}/(M_\kappa M_{\kappa'})^{1/2} \tag{2}$$

where α and β indices label the Cartesian coordinates, and κ and κ' run over all the atoms in the unit cell with ionic masses of M_κ and $M_{\kappa'}$, respectively; and $\widetilde{C}$ is Fourier transform of interatomic force constant and can be obtained as second derivative of total energy with respect to collective atomic displacements. A standard group theoretical analysis indicates that the modes at zone center can be decomposed as

$$\Gamma_{\text{vib}} = 30A_1 \oplus 30A_2 \oplus 30B_1 \oplus 30B_2 \tag{3}$$

Of the 120 modes, 87 modes ($29A_1 + 29B_1 + 29B_2$) are both Raman-active and IR-active and $30A_2$ modes are only Raman-active, the remaining three modes being the zero frequency translational modes. Our calculated phonon frequencies with their irreducible representation are listed in Table 3 and Fig. 1 presents a graphical presentation of the position of eigenfrequencies for each symmetry representation. For IR-active modes there are LO–TO splittings due to the coupling of the atomic displacement with the long-range electric field by means of the Born effective charge tensor. It can be seen from Table 3 that these splittings, as expected from the small difference between the Born effective charge of each atom and its nominal ionic valence, are small. A comparison between these phonon frequencies with experiment is not feasible since, to our knowledge, there are not corresponding experimental data. However, our results can play an important role in mode assignment of κ-Al_2O_3.

The static dielectric permittivity tensor $\varepsilon^0_{\alpha\beta}$ can be obtained by adding to $\varepsilon^\infty_{\alpha\beta}$, the ionic contribution according to

$$\varepsilon^0_{\alpha\beta} = \varepsilon^\infty_{\alpha\beta} + \frac{4\pi}{\Omega_0} \sum_m \frac{\left(\sum_{\kappa\alpha'} Z^*_{\kappa,\alpha\alpha'} U^*_m(\kappa\alpha')\right)\left(\sum_{\kappa'\beta'} Z^*_{\kappa',\beta\beta'} U_m(\kappa\beta')\right)}{\omega_m^2} \tag{4}$$

where Ω_0 is the volume of the primitive unit cell, and U_m and ω_m are eigendisplacement and frequency of the mth IR-active phonon normal mode, respectively. We find

$$\begin{pmatrix} 11.756 & 0 & 0 \\ 0 & 11.356 & 0 \\ 0 & 0 & 12.040 \end{pmatrix} \tag{5}$$

The calculated static dielectric permittivity tensor has the correct form expected from the crystal point group; it is diagonal with $\varepsilon_{xx} \neq \varepsilon_{yy} \neq \varepsilon_{zz}$. Once again, a direct comparison of this dielectric tensor with experiment is not feasible since, to our knowledge, there are not experimental data for κ-Al_2O_3. A comparison of our result can be made with amorphous Al_2O_3. Our orientationally

Table 3
Calculated phonon frequencies (in cm^{-1}) of κ-Al_2O_3

A_1			B_1			B_2			A_2	
Mode	TO	LO	Mode	TO	LO	Mode	TO	LO	Mode	
1	135.28	137.21	1	166.10	173.86	1	184.56	185.21	1	146.37
2	185.21	187.68	2	198.87	199.35	2	229.19	234.66	2	173.86
3	204.68	213.64	3	248.95	248.96	3	261.26	263.97	3	213.64
4	247.24	247.39	4	285.27	285.30	4	290.31	291.57	4	240.48
5	270.03	270.20	5	300.44	303.15	5	293.30	293.99	5	267.60
6	284.70	285.27	6	323.51	323.52	6	313.18	314.33	6	292.33
7	304.30	309.27	7	331.99.	334.05	7	321.14	323.51	7	309.27
8	317.84	321.14	8	348.53	348.94	8	353.75	354.99	8	329.87
9	338.14	341.71	9	354.99	355.61	9	373.37	384.28	9	346.15
10	393.77	394.22	10	394.22	400.05	10	392.22	393.30	10	356.38
11	406.72	409.42	11	400.81	406.32	11	412.02	412.30	11	389.98
12	411.16	412.02	12	412.30	424.03	12	444.50	445.06	12	406.32
13	445.31	445.43	13	426.65	429.97	13	451.45	452.51	13	452.51
14	467.96	469.62	14	440.89	444.50	14	476.88	478.00	14	467.45
15	483.97	491.34	15	456.07	465.67	15	494.92	499.38	15	474.67
16	499.38	510.25	16	482.07	482.20	16	521.92	526.36	16	478.00
17	520.40	521.92	17	491.34	491.35	17	534.48	538.04	17	493.50
18	540.56	540.87	18	528.09	532.34	18	553.90	555.26	18	540.87
19	550.09	553.90	19	542.48	546.67	19	561.60	565.78	19	546.67
20	565.78	569.76	20	580.73	584.08	20	584.08	596.80	20	555.26
21	606.76	608.03	21	617.85	625.03	21	613.51	617.85	21	603.37
22	608.06	613.51	22	631.29	646.46	22	646.46	657.56	22	628.07
23	658.19	676.04	23	676.04	685.45	23	685.45	685.46	23	657.56
24	710.96	720.51	24	731.26	743.86	24	698.08	704.28	24	692.08
25	724.91	730.46	25	755.35	756.58	25	720.86	721.94	25	704.28
26	730.55	731.26	26	761. 11	765.78	26	753.89	755.35	26	720.50
27	769.32	769.74	27	800.23	802.76	27	769.77	778.83	27	745.20
28	778.83	798.33	28	818.27	820.61	28	798.33	800.33	28	765.78
29	828.01	845.76	29	901.32	932.35	29	820.61	828.01	29	802.76
									30	845.76

A_1, B_1 and B_2 are both Raman-active and IR-active. A_2 modes are Raman-active.

averaged static dielectric constant of 11.71 agrees reasonably well with the result of Fig. 7 in Ref. [4] which report dielectric constant of alumina in amorphous phase (before densification due annealing at temperatures greater than 800 °C, where Al_2O_3 layer is amorphous; see Fig. 5 and Fig. 8 of Ref. [4]) to be approximately 11. The difference is about 6.5%, as often found in the local-density approximation to the density-functional theory. Here we compare the value of ionic contribution to static dielectric constant of κ-Al_2O_3 with the corresponding experimental value of amorphous Al_2O_3. Our calculated orientationally averaged value of ionic contribution to static dielectric constant (ε_{ion}^{ave}) of κ-Al_2O_3 is 8.543. To compare this value with experimental value of ionic contribution to static dielectric constant (ε_{ion}) of amorphous Al_2O_3, we subtract the experimental value of $\varepsilon_\infty = 2.756$, which can be estimated from index of refraction that has been reported in Fig. 8 of Ref. [4] to be 1.66 for as deposited and annealed (up to 800 °C) film (i.e. amorphous phase), from experimental value of $\varepsilon_0 = 11$. We find that our calculated ε_{ion}^{ave} of κ-Al_2O_3 is in good agreement with the experimental value $\varepsilon_{ion} = 8.244$ of amorphous Al_2O_3; the difference is about 3.62%. On the other hand the ε_{ion}^{ave} of α-Al_2O_3 (another phase of Al_2O_3 which has Al atoms only in the octahedral coordination with O atoms) is 7.097, as can be obtained from the results that have been reported in previous theoretical work of Ref. [27]. The difference of this value with the experimental value

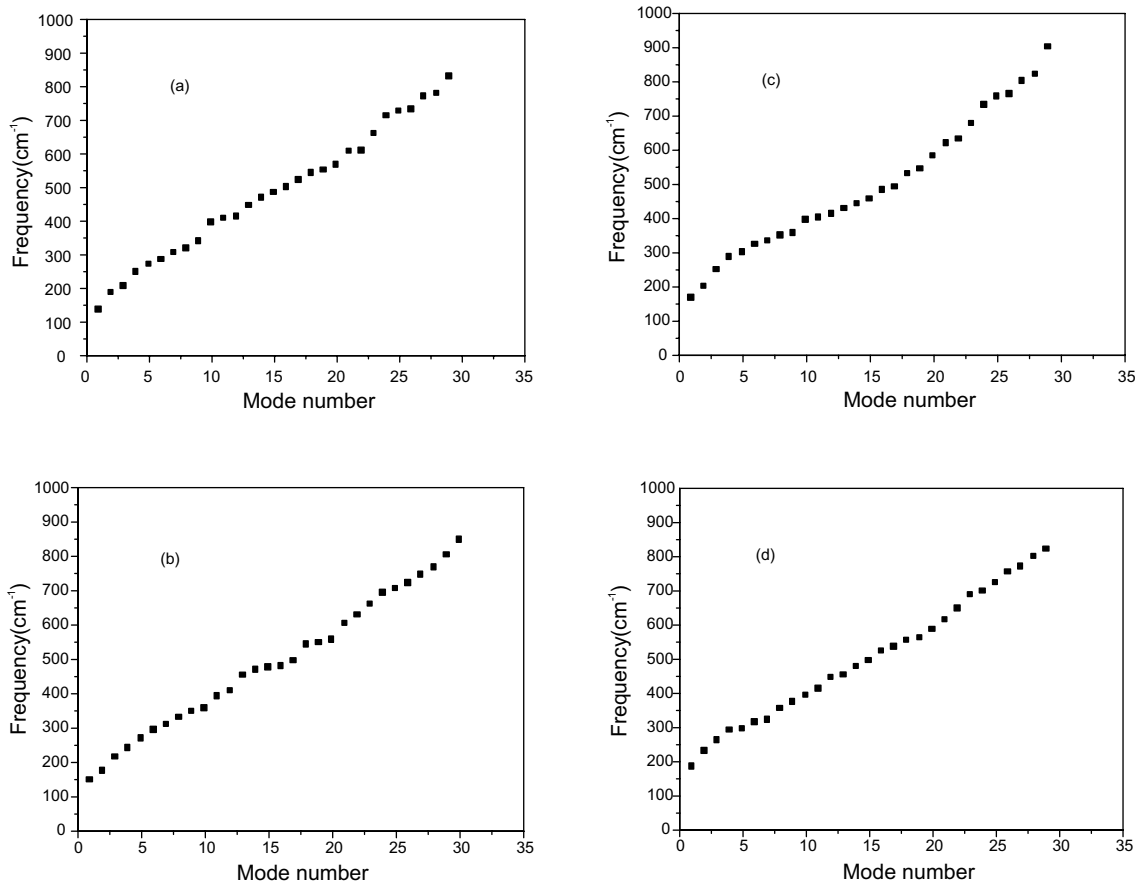

Fig. 1. Graphical presentation of the position of eigenfrequencies for (a) A_1, (b) A_2, (c) B_1, (d) B_2, symmetry representation.

$\varepsilon_{ion} = 8.244$ of amorphous Al_2O_3 is about 13.9%. These results, together with the fact that κ-Al_2O_3 and amorphous Al_2O_3, similarly have Al atoms in both octahedral and tetrahedral coordination with O atoms while α-Al_2O_3 has Al atoms only in octahedral coordination with O atoms, demonstrate the coordination dependence of ionic contribution to static dielectric constant of Al_2O_3; the ioniccontribution to static dielectric constant decreases with increasing of coordination of Al with O atoms.

Also our calculated orientationally averaged electronic dielectric constant of κ-Al_2O_3 ($\varepsilon_{ele}^{ave} = 3.167$) is in excellent agreement with the corresponding value of α-Al_2O_3 ($\varepsilon_{ele}^{ave} = 3.166$), as can be obtained from theoretical results of Ref. [27].

4. Conclusion

We have investigated the structural, dynamical, and dielectric properties of κ-Al_2O_3 within density-functional theory. The parameters of relaxed atomic structure are found to be in very good agreement with experimental data. The Born effective charge tensors, the phonon frequencies at the center of the Brillouin zone, and the electronic and static dielectric permittivity tensors have been obtained using density-functional perturbation theory. The Born effective charges are close to their nominal values, indicating the nearly ionic bonding in this system. The computed phonon frequencies can be used in mode assignment of κ-Al_2O_3. The obtained electronic and static dielectric

permittivity tensors have the correct form expected from crystal point group. Although a direct comparison of calculated static dielectric permittivity tensor with experiment is not feasible, but its orientationally averaged value agree reasonably well with the available experimental ε_0 of amorphous alumina. Especially, the calculated orientationally averaged ionic contribution to static dielectric constant of κ-Al_2O_3 is in good agreement with the experimental value of ionic contribution to static dielectric constant of amorphous Al_2O_3. Also using our calculated ionic contribution to static dielectric constant of κ-Al_2O_3, together with the previous theoretical results of α-Al_2O_3 and available experimental data of amorphous Al_2O_3, we demonstrate that the ionic contribution to static dielectric constant of Al_2O_3 decreases with increasing of coordination of Al with O atoms.

Acknowledgements

We would like to acknowledge Professor X. Gonze (Université Catholique de Louvain) and other contributors for the availability of the ABINIT code.

References

[1] Internat. Technol. Roadmap for Semiconductors, Semiconductor Association, San Jose, 1999.
[2] H.S. Momose, M. Ono, T. Yoshitomi, T. Ohguro, S.I. Naakamure, M. Saito, H. Iwai, IEEE Trans. Electron Dev. 43 (1996) 1233.
[3] J.P. Chang, Y.-S. Lin, Appl. Phys. Lett. 79 (2001) 3666.
[4] E.P. Gusev, E. Cartier, D.A. Buchanan, M. Gribelyuk, M. Copel, H. Okorn-Schmidta, C. D'Emic, Microelectron. Eng. 59 (2001) 341.
[5] C.C. Liao, A. Chin, C. Tasi, J. Crystal Growth 201 (1999) 652.
[6] M. Copel, E. Cartier, E.P. Gusev, S. Guhan, N. Bojarczuk, M. Poppeler, Appl. Phys. Lett. 78 (2001) 2670.
[7] R. Ludeke, M.T. Cuberes, E. Cartier, Appl. Phys. Lett. 76 (2001) 2886.
[8] S. Guha, E. Cartier, M.A. Gribelyuk, N.A. Bojarczuk, M.C. Copel, Appl. Phys. Lett. 77 (2000) 2710.
[9] J. Kwo, M. Hong, A.R. Kortan, K.T. Queeney, Y.J. Chabal, J.P. Mannaerts, T. Boone, J.J. Krajewski, A.M. Sergent, J.M. Rosamilia, Appl. Phys. Lett. 77 (2000) 130.
[10] G.D. Wilk, R.M. Wallace, Appl. Phys. Lett. 76 (2000) 112.
[11] B. Ollivier, R. Retoux, P. Lacorre, D. Massiot, G. Ferey, J. Mater. Chem. 7 (1997) 1049.
[12] S. Daviero, A. Ibanez, C. Avinens, A.M. Flank, Thin Solid Films 226 (1993) 207.
[13] X. Gonze, J.-M. Beuken, R. Caracas, F. Detraux, M. Fuchs, G.-M. Rignanese, L. Sindic, M. Verstraete, G. Zerah, F. Jollet, M. Torrent, A. Roy, M. Mikami, Ph. Ghosez, J.-Y. Raty, D.C. Allan, Comput. Mater. Sci. 25 (2002) 478.
[14] W. Kohn, L.J. Sham, Phys. Rev. 140 (1965) A1133.
[15] S. Goedecker, SIAM (Soc. Ind. Appl. Math.) J. Sci. Stat. Comput. 18 (1997) 1605.
[16] M.C. Payne, M.P. Teter, D.C. Allan, T.A. Arias, J.D. Joannopoulos, Rev. Mod. Phys. 64 (1992) 1045.
[17] X. Gonze, Phys. Rev. B 54 (1996) 4383.
[18] P. Hohenberg, W. Kohn, Phys. Rev. 136 (1964) B864.
[19] D.M. Ceperley, B.J. Alder, Phys. Rev. Lett. 45 (1980) 566.
[20] S. Goedecker, M. Teter, J. Hutter, Phys. Rev. B 54 (1996) 1703.
[21] N. Troullier, J.L. Martins, Phys. Rev. B 43 (1991) 1993.
[22] H.J. Monkhorst, J.D. Pack, Phys. Rev. B 13 (1976) 5188.
[23] X. Gonze, D.C. Allan, M.P. Teter, Phys. Rev. Lett. 68 (1992) 3603.
[24] X. Gonze, Phys. Rev. B 55 (1997) 10337.
[25] X. Gonze, C. Lee, Phys. Rev. B 55 (1997) 10355.
[26] S. Baroni, S. de Gironcoli, A. Dal Corso, P. Giannozzi, Rev. Mod. Phys. 73 (2001) 515.
[27] R. Heid, D. Strauch, K.-P. Bohnen, Phys. Rev. B 61 (2000) 8625.